

## Fissionlike Decay of $^{20}\text{Ne}$ : Eccentric Behavior in the B + B Fusion Processes

A. Szanto de Toledo, M. M. Coimbra, N. Added, R. M. Anjos, N. Carlin Filho, L. Fante, Jr.,  
M. C. S. Figueira, V. Guimarães, and E. M. Szanto

*Departamento de Física Nuclear, Laboratório Pelletron, Instituto de Física da Universidade de São Paulo,  
CP 20516 01489 São Paulo, São Paulo, Brazil*

(Received 5 October 1988)

Cross sections for fusion of  $^{10,11}\text{B} + ^{10,11}\text{B}$  have been measured in the energy range from 1.5 to 5 MeV/nucleon. The  $^{10}\text{B} + ^{10}\text{B}$  system unexpectedly presents a hindered fusion cross section when compared to the  $^{10}\text{B} + ^{11}\text{B}$  and  $^{11}\text{B} + ^{11}\text{B}$  reactions and to standard-model predictions. The missing fusion cross section was diverted to the  $^{10}\text{B}$  exit channel with a total kinetic energy characteristic of strongly damped collisions.  $Q$  values and kinematical analysis together with angular distributions suggest a binary symmetric decay of the composite  $^{20}\text{Ne}$  system.

PACS numbers: 25.70.Jj, 25.70.Gh, 25.70.Lm

Systematic studies of fusion reactions of medium-weight nuclei have revealed that the macroscopic characteristics of the colliding nuclei and resulting compound nucleus are the determinants in the fusion-cross-section limitation.<sup>1,2</sup> However, when light nuclei such as the  $2s-1p$  shell nuclei are involved, systematic descriptions become very difficult to establish.<sup>3-5</sup> The understanding of the mechanism responsible for the inhibition of compound-nucleus formation in the lighter systems is further complicated by the influence that the structures of the participant nuclei exert in the process and by the large variety of important and competing reaction mechanisms which prevail.

On the other hand, collisions between light nuclei allow the formation of a variety of composite systems with comparable size and angular momentum but with significant differences in their excitation energies, resulting from the large variation that the binding energy can undergo when a single nucleon is added.

Because the binding energy per nucleon for light nuclei has not yet reached saturation and the Coulomb and centrifugal repulsive forces have not as yet significantly surpassed the attractive nuclear force, the amalgamation of the collision participants becomes a very probable channel, and the subsequent fission into two complex fragments is severely restricted.

In this Letter, we report on the observation of a definite inhibition of the fusion cross section for the  $^{10}\text{B} + ^{10}\text{B}$  system and a significant cross section of fissionlike reaction products, in contrast to an appreciable fusion cross section with the lack of such an intense outgoing channel in both the  $^{11}\text{B} + ^{11}\text{B}$  and  $^{11}\text{B} + ^{10}\text{B}$  reactions.

In the experiment,  $^{10,11}\text{B}$  self-supporting targets were bombarded by  $^{10,11}\text{B}$  beams from the University of São Paulo Pelletron Accelerator. The bombarding energies ranged from 15 to 50 MeV. Light, charged reaction products and evaporation residues were identified by means of a position-sensitive ionization chamber. Angu-

lar distributions ranging from  $\theta_{\text{lab}} = 5^\circ$  to  $45^\circ$  were measured in steps of  $1^\circ$  along with excitation functions at five forward angles. Complete elastic-scattering angular distributions ( $24 \text{ MeV} < E_{\text{lab}} < 48 \text{ MeV}$ ,  $\Delta E_{\text{lab}} = 8 \text{ MeV}$ , and  $15^\circ \leq \theta_{\text{c.m.}} \leq 120^\circ$ ,  $\Delta\theta = 1^\circ$ ) were also measured using the kinematical coincidence technique. Fits to these elastic angular distributions supplied optical-model parameters and total reaction cross sections for the three systems investigated.

Reaction products<sup>6</sup> were distinguished by comparing the velocity spectra for the  $Z=5$  to 9 elements to those expected for the evaporation residues and the transferred particles with optimum  $Q$  values, respectively.

Spectra for the elements  $Z=6$  and 7, in which evaporation residues and direct-reaction components were simultaneously present, were unfolded by subtracting from the experimental spectra the predicted evaporation-residue spectra generated by Monte Carlo-Hauser-Feshbach calculations performed by the code LILITA,<sup>7</sup> renormalized to the data using the structure present in the data itself as a guide. The structure of the resulting spectrum has been associated with a direct-reaction process and described by a  $Q$  window centered at an optimum  $Q_{\text{opt}}$  value with a width given by Ref. 8. With this procedure the direct component is identified. The remaining cross section from the original spectrum was consequently attributed to the evaporation-residue cross section.

Thus the deduction of the absolute cross sections for  $Z=6$  and 7 elements is essentially independent of the statistical-model calculations, and confidence in this unfolding procedure is further provided by the agreement of the angular distributions for both processes with their model predictions.<sup>7</sup>

Fits of the measured excitation functions by the Glas-Mosel model<sup>9</sup> supplied values of  $R_{\text{cr}}$  ( $R_B$ ) and  $V_{\text{cr}}$  ( $V_B$ ) for the critical (barrier) radii and potential strengths which are compatible with the systematics of this mass region.<sup>1,10</sup> These values were used in the determination

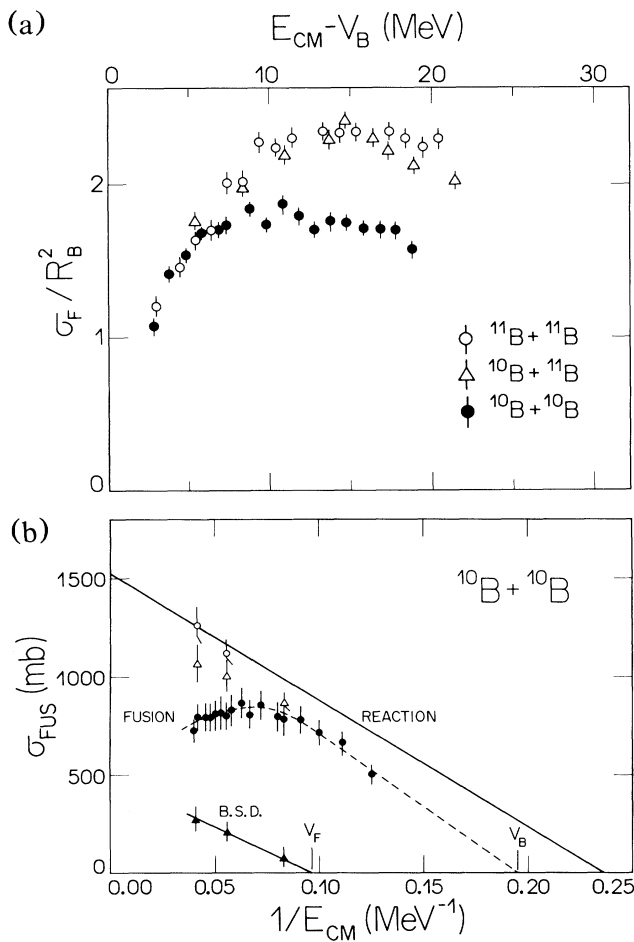


FIG. 1. (a) Reduced fusion cross sections obtained using the barrier parameters [ $R_B$  (fm);  $V_B$  (MeV)] = [6.81;5.16], [6.80;4.65], and [7.12;4.62] for the  $^{10}\text{B} + ^{10}\text{B}$ ,  $^{10}\text{B} + ^{11}\text{B}$ , and  $^{11}\text{B} + ^{11}\text{B}$  reactions, respectively. (b) Experimental cross sections of the  $^{10}\text{B} + ^{10}\text{B}$  reactions: Evaporation residues (closed circles), BSD fragments (closed triangles), and their sum (open triangles). The sum including the measured quasielastic cross section is represented by open circles.  $V_F$  represents the BSD process threshold. The dashed line represents a fit by the Glas-Mosel model and the solid line corresponds to the derived total reaction cross section.

of the reduced fusion cross sections  $\sigma_F/R_B^2$  shown in Fig. 1(a) for which most of the macroscopic effects of the entrance channel on the fusion cross section are removed, consequently enhancing any possible anomalous behavior of a particular system. In fact, the  $^{10}\text{B} + ^{10}\text{B}$  system displays a significantly hindered cross section ( $\approx 40\%$  lower than for the other two reactions) and as a consequence, a lower critical angular momentum. A detailed investigation of the velocity-converted spectra of the  $Z=5$  products (Fig. 2) reveals that a broad structure is clearly present, with an average velocity larger than that expected for an evaporation residue of the  $^{20}\text{Ne}$  com-

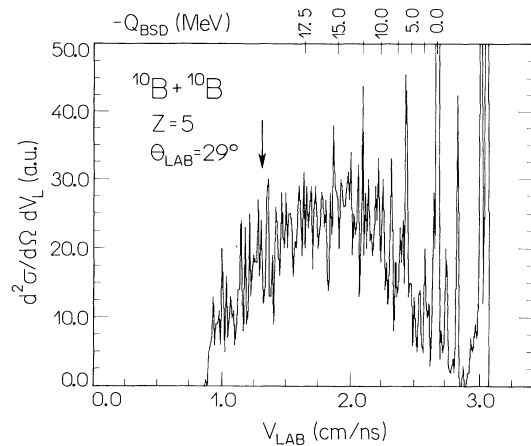


FIG. 2. Velocity-converted spectrum of the  $Z=5$  elements from the  $^{10}\text{B} + ^{10}\text{B}$  reaction at  $E_{lab} = 48$  MeV. The upper scale refers to the corresponding  $Q_{BSD}$  value assuming the binary symmetric decay channel for the  $^{20}\text{Ne}$  compound nucleus. The vertical arrow corresponds to the compound-nucleus recoil velocity  $V_{CN} \cos\theta_{lab}$ .

pound nucleus. The analysis of the angular dependence of the velocity centroid of these structures describes a circle centered at the compound-nucleus velocity [see Fig. 3(a)], and suggests the occurrence of a binary process with a symmetric splitting of the composite nucleus. Measurements<sup>11</sup> of the evaporation residues' time of flight reveal that they correspond to  $^{10}\text{B}$ .

Displayed in Fig. 1(b) are the total fusion cross sections for the  $^{10}\text{B} + ^{10}\text{B}$  system and the cross section for binary symmetric decay (BSD). The sum of all the processes observed, including the quasielastic processes, exhausts the total reaction cross section. The threshold  $V_F \approx 11$  Mev for BSD is of the order of the fission barrier height predicted recently by Sierk<sup>12</sup> and by Mustafa *et al.*<sup>13</sup> for the critical angular momentum. Liquid-drop-model (LDM) predictions for nuclei as light as  $^{20}\text{Ne}$  may carry large uncertainties when the neglected shell effects become relevant and when light nuclei are described as sharp-surfaced liquid drops.<sup>12-14</sup> However, the consistency observed supports the picture of the dynamical scission of the rotating composite nucleus, which attains a very deformed configuration at relatively low angular momenta ( $\leq 12\hbar$ ).

At the bombarding energies at which angular distributions were measured, a most probable  $Q_{BSD}$  value was extracted and no dependence on the detection angle has been observed. The angular distributions of these  $Z=5$  products were found to reflect an isotropic emission probability ( $d\sigma/d\Omega \propto 1/\sin\theta$ ) indicating that the composite nucleus survived longer than a single rotation period before scission occurred [see Fig. 3(b)]. This BSD process has been pursued in the other reactions investigated. No evidence in the  $^{11}\text{B} + ^{11}\text{B}$  channel has been found, thus allowing an upper limit to its cross sec-

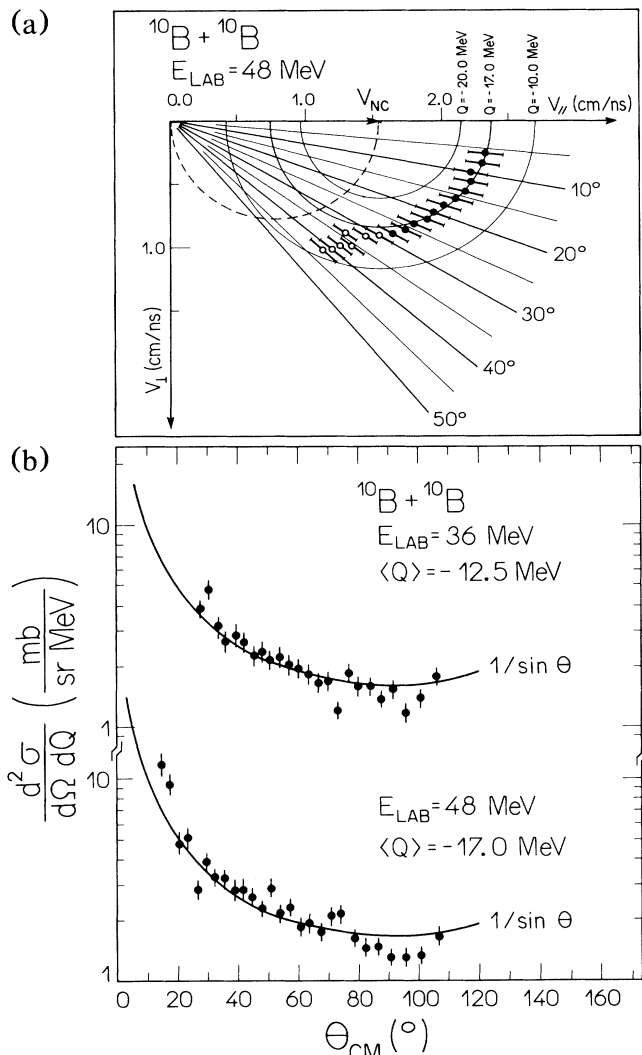


FIG. 3. (a) Experimental average velocities for the  $Z=5$  fissionlike products (closed circles). Cases in which electronic cutoff in the velocity spectrum exists are indicated by the open circles. The dashed line indicates the expected evaporation residues' velocities, and the solid lines indicate the fragments' velocities for the BSD with  $Q$  values indicated. (b) Angular distributions of the  $Z=5$  spectra for a 1-MeV bin centered at the most probable  $\langle Q \rangle$  value, for the  $^{10}\text{B}+^{10}\text{B}$  reaction at two different bombarding energies.

tion to be estimated. In the case of the  $^{10}\text{B}+^{11}\text{B}$  channel, it has been possible to characterize clearly the BSD process only at the highest energy investigated.

The magnitudes of the measured cross sections for this fissionlike process (at  $E_{\text{lab}}=48$  Mev,  $\sigma_{\text{BSD}} \approx 270$  mb for the  $^{10}\text{B}+^{10}\text{B}$  channel,  $< 130$  mb for the  $^{10}\text{B}+^{11}\text{B}$  channel, and  $< 70$  mb for the  $^{11}\text{B}+^{11}\text{B}$  channel) are at least a factor of 20 larger than the predictions for the fusion-fission cross section based on Hauser-Feshbach calculations. They were performed using the codes STATIS,<sup>15</sup>

CASCADE,<sup>16</sup> and PACE<sup>17</sup> which makes use of the Sierk fission barriers.<sup>12</sup> Furthermore, 95% of the  $Z=5$  yield predicted by Monte Carlo calculations for the  $^{10}\text{B}+^{10}\text{B}$  system belongs to the  $^{11}\text{B}$  isotope while the observed yield is due to  $^{10}\text{B}$ . The observed velocity shifts of these fully damped fragments, when compared to the velocity of the residues of a sequential evaporation of  $\alpha$  particles (i.e., *aap* channel), cannot be accounted for, even if high-energy  $\alpha$  particles were evaporated very anisotropically. However, an enhanced statistical emission of heavy fragments could justify this shift.

The production of lithium and beryllium in very light heavy-ion reactions has been investigated<sup>18,19</sup> and it has been shown that the mechanism is predominantly compound. The magnitude of the observed cross section is very low and would not account, in the case of a Li- $\alpha$  sequential emission, for the observed  $^{10}\text{B}$  yield. This has been verified by means of detailed Hauser-Feshbach calculations for Li and Be evaporation which predict at most a total cross section of the order of 10 mb for the  $^{10}\text{B}+^{10}\text{B}$  system at 48 MeV for a first-chance lithium emission. Further arguments strongly restrict the possibility of a significant Li evaporation chain: the facts that the total observed lithium cross section is of the order of 196 mb at 48 MeV (i.e., smaller than the 270 mb for fissionlike products) and that the analysis of the Li energy spectra and angular distributions suggests that direct processes can be considered, for which projectile breakup is the main component.

A significant  $^6\text{Li}$  and  $^{10}\text{B}$  contribution associated with the  $\alpha$  decay of  $^{14}\text{N}$  produced in the  $^{10}\text{B}(^{10}\text{B},^6\text{Li})^{14}\text{N}$  reaction can be ruled out because of the observed values of the  $^{10}\text{B}$  kinetic energy when compared to the expected most probable energy associated to a  $Q_{\text{opt}}$  value for the process. Furthermore, for these energies the reaction kinematics impose an angular limit for  $^{10}\text{B}$  which is much smaller than those observed. Finally, it should be noted that for this transfer reaction an angular distribution proportional to  $1/\sin\theta$  is *not* expected (Fig. 3) even though the identical-particle nature of the entrance channel imposes an angular distribution symmetric around  $90^\circ$ .

Recent studies<sup>20-24</sup> of collisions between medium-weight nuclei have revealed the existence of a yield resulting from the breakup of a dinuclear system, associated with a strongly damped collision. An interpretation based on the statistical decay of a dinuclear doorway configuration characterized by an orbiting<sup>25</sup> process has been successful in describing measured cross sections. These models were applied for the fusion and possible "orbiting" of the B+B systems. Although the cross section of 160 mb predicted for the integrated orbiting yield for the  $^{10}\text{B}+^{10}\text{B}$  reaction at  $E_{\text{lab}}=48$  MeV is of the right order of magnitude (i.e., approximately a factor of 2 smaller) this model predicts that a significant yield (i.e.,  $\approx 140$  mb) should be observed in the  $^{11}\text{B}+^{11}\text{B}$  re-

action at the same bombarding energy, a feature which is not observed experimentally.

The picture of a composite dinuclear  $^{20}\text{Ne}$  system splitting at higher angular momenta is further supported by analyzing the energy surface in the  $\beta$ - $\gamma$  plane based on Strutinsky-type calculations<sup>26</sup> for the  $^{20}\text{Ne}$  and  $^{22}\text{Ne}$  yrast states. The trajectories of the yrast states shown in Ref. 26 indicate that the  $^{20}\text{Ne}$ , in spite of being a comparatively more compact nucleus is, at higher angular momenta, a far more softer nucleus which suffers a sudden deformation from  $\beta=0.1$  to 0.6, becoming nearly prolate when states with  $J=14\hbar$  are populated. This fact is not expected in the case of  $^{22}\text{Ne}$ .

Although in the present work the mass distributions of the fissionlike products appear to be a very narrow band due to the low compound-nucleus excitation energy, additional experiments, to determine precise mass distributions and to establish the systematics of the symmetric splitting of very light systems, are advisable in order to clarify this rarely observed and still poorly understood phenomenon. Furthermore, this would also contribute to the understanding of the behavior of light nuclei at high-spin states and the role that nuclear structure characteristics plays in collision dynamics.

The authors wish to thank Professor E. Farrelly-Pessoa for the critical reading of the manuscript. A.S.d.T. and E.M.S. were supported in part by Conselho Nacional de Desenvolvimento Científico e Tecnológico (CNPq), Brazil. M.M.C., N.A., R.M.A., M.C.S.F., and V.G. were supported by Fundação de Amparo e Pesquisa do Estado de São Paulo (FAPESP), Brazil. L.F. was supported by CNPq.

<sup>1</sup>D. G. Kovar *et al.*, Phys. Rev. C **20**, 1305 (1979).

<sup>2</sup>S. G. Steadman *et al.*, Annu. Rev. Nucl. Part. Sci. **36**, 649 (1986).

<sup>3</sup>J. Gomez del Campo *et al.*, Phys. Rev. C **29**, 1722 (1984).

<sup>4</sup>J. F. Mateja *et al.*, Phys. Rev. C **33**, 1649 (1986); **33**, 1307 (1986); J. F. Mateja *et al.*, Phys. Rev. C **30**, 134 (1984).

<sup>5</sup>J. Gomez del Campo *et al.*, Phys. Rev. C **35**, 137 (1987).

<sup>6</sup>M. M. Coimbra *et al.*, Ph.D. thesis, University of São Paulo, 1988 (unpublished); (to be published).

<sup>7</sup>J. Gomez del Campo, Phys. Rev. C **19**, 2170 (1979); Monte Carlo code LILITA, Oak Ridge National Laboratory Report No. ORNL/TM 7235, 1981 (unpublished).

<sup>8</sup>T. Kammuri *et al.*, Nucl. Phys. **A366**, 171 (1981), and references therein.

<sup>9</sup>D. Glas *et al.*, Nucl. Phys. **A237**, 429 (1975).

<sup>10</sup>O. Civitarese *et al.*, Phys. Lett. **125B**, 22 (1983).

<sup>11</sup>A. Szanto de Toledo *et al.* (to be published).

<sup>12</sup>A. J. Sierk, Phys. Rev. C **33**, 2039 (1986).

<sup>13</sup>M. G. Mustafa *et al.*, Phys. Rev. C **25**, 2524 (1982).

<sup>14</sup>J. Blocki *et al.*, Nucl. Phys. **A445**, 367 (1985).

<sup>15</sup>R. G. Stokstad, STATIS, Wright Nuclear Structure Laboratory, Yale University Internal Report No. 52, 1972 (unpublished).

<sup>16</sup>F. Pühlhofer, CASCADE, Gesellschaft für Schwerionenforschung Darmstadt report, 1979 (unpublished); Nucl. Phys. **A280**, 267 (1977).

<sup>17</sup>A. Gavron, PACE, Phys. Rev. C **21**, 230 (1980).

<sup>18</sup>R. G. Stokstad *et al.*, Phys. Rev. C **16**, 2249 (1977).

<sup>19</sup>D. L. Hanson *et al.*, Phys. Rev. C **9**, 929 (1974).

<sup>20</sup>D. Shapira *et al.*, Phys. Lett. **114B**, 111 (1982).

<sup>21</sup>D. Shapira *et al.*, Phys. Rev. Lett. **53**, 1634 (1984), and references therein.

<sup>22</sup>K. Grotowski *et al.*, Phys. Rev. C **30**, 1214 (1984).

<sup>23</sup>A. Glaesner *et al.*, Phys. Lett. **169B**, 153 (1986).

<sup>24</sup>M. S. Hussein *et al.*, Phys. Rev. Lett. **54**, 2659 (1985); B. V. Carlson *et al.*, Ann. Phys. (N.Y.) **169**, 167 (1986).

<sup>25</sup>B. Shivakumar *et al.*, Phys. Rev. C **35**, 1730 (1987).

<sup>26</sup>E. M. Szanto *et al.*, Phys. Rev. Lett. **42**, 622 (1979); Nucl. Phys. **A404**, 142 (1983).